

Increasing molecular O₃ storage capacity in a clathrate hydrate

 Kazutoshi Shishido,^a Sanehiro Muromachi,^b Ryo Nakamura,^a Satoshi Takeya^b and Ryo Ohmura^{*a}

 Cite this: *New J. Chem.*, 2014, **38**, 3160

 Received (in Montpellier, France)
8th November 2013,
Accepted 13th March 2014

DOI: 10.1039/c3nj01377d

www.rsc.org/njc

This paper reports an experimental study to further increase the ozone storage capacity in a clathrate hydrate and to better understand the relationship between the gas phase O₃ concentration and the O₃ storage capacity in the hydrate. We performed experiments with the O₃ + O₂ + CO₂ feed gas with an increased O₃ fraction in the gas phase exceeding that covered by a preceding study. To accurately specify the thermodynamic conditions to form the hydrate, we first measured the three-phase (gas + liquid + hydrate) equilibrium conditions for the (O₃ + O₂ + CO₂ + H₂O) and (O₂ + CO₂ + H₂O) systems. The phase equilibrium data cover the temperature range from 272 to 277 K, corresponding to pressures from 1.6 to 3.1 MPa, for each of the two different (O₃ + O₂)-to-CO₂ or O₂-to-CO₂ molar ratios in the feed gas, which are approximately 4 : 6 and 5 : 5, respectively. The O₃ fraction in the gas phase was ~0.025. Based on the equilibrium data, we prepared crystal samples of the O₃ + O₂ + CO₂ hydrates at a system pressure of 3.0 MPa and a temperature of 272 K. The highest O₃ storage capacity in the hydrates was measured to be 2.15 mass% which is 2.36 times higher than the highest past record of 0.91 mass%. The results also show that the dominant factor to control the O₃ storage capacity in the hydrates is the O₃ mole fraction in the gas phase in contact with the hydrates.

Introduction

Ozone (O₃) is a strong oxidant which causes only slight environmental damage because of its nature of decomposing to oxygen (O₂). Based on these advantages, there are various applications of ozone in industry, *e.g.*, purification of water and sterilization of perishables. However, since the decomposition reaction to oxygen occurs spontaneously, ozone is difficult to preserve. Thus, in order to use ozone in industry, it has been generated by an onsite ozone generator which is a costly device. To establish ozone preservation technology, experimental and theoretical studies of O₃-containing clathrate hydrates have recently been reported.^{1–4}

Clathrate hydrates are crystalline solids consisting of “host” water molecules which compose cages and “guest” molecules enclosed in the cages. Ozone molecules can be separated from each other by the hydrate cage walls and thus prevented from mutually interacting to cause the ozone-to-oxygen reaction. Based on this nature, the idea of storing ozone using hydrates was first proposed by McTurk and Waller⁵ in 1964. This technology provides an ozone density 100 to 1000 times higher

than that of modern ones such as ozonated water and ozonated ice. In the patent application document,³ it is shown that hydrate formation from an O₃ + O₂ gas mixture would require a high pressure and a low temperature, *e.g.*, 13 MPa and 248 K. To decrease the hydrate-forming pressure, it is effective to use an appropriate second guest substance which is called a *help* guest. If the simple hydrate of the *help* guest is formed under milder conditions compared to the hydrate of the main-target guest substance, adding the second guest as the *help* guest in the feed gas would form a double hydrate containing the main and *help* guests under milder conditions.⁶ The *help* guest needs to have sufficient chemical durability against ozone oxidation. As such *help* guests, carbon tetrachloride, xenon, 1,1-dichloro-1-fluoro-ethane and carbon dioxide were previously tested.^{7–9} Due to the toxicity of carbon tetrachloride, the cost of xenon and the environmental impacts of 1,1-dichloro-1-fluoro-ethane, we selected carbon dioxide as the most promising substance in place of the other *help* guests.

For practical use of the O₃-containing hydrates, it is necessary to determine the thermophysical properties relevant to these hydrates. Muromachi *et al.*¹⁰ performed three-phase (gas + liquid + hydrate) equilibrium measurements for the O₃ + O₂ + CO₂ + H₂O systems. These data cover the temperature range from 272 K to 279 K, corresponding to pressures up to 4 MPa, for each of the (O₃ + O₂)-to-CO₂ or O₂-to-CO₂ molar ratios in the feed gas, which are approximately 1 : 9, 2 : 8, and 3 : 7. The concentration of ozone in

^a Department of Mechanical Engineering, Keio University, Yokohama 223-8522, Japan. E-mail: rohmura@mech.keio.ac.jp

^b National Institute of Advanced Industrial Science and Technology (AIST), Tsukuba 305-8569, Japan



the $O_3 + O_2$ mixture was less than 11 mol%. Nakajima *et al.*² performed the measurements for the O_3 storage capacity in the $O_3 + O_2 + CO_2$ hydrates formed from four different $O_3 + O_2$ versus CO_2 molar ratios (1 : 9, 2 : 8, 3 : 7, 4 : 6) in the feed gas. The O_3 storage capacity was evaluated as an ozone mass fraction in the hydrate because the mass of the storage media had an impact on the storage and transportation efficiency. Their hydrate samples were prepared at system pressures of 2.0, 2.5 and 3.0 MPa and a temperature of 272 K. The results of these tests also showed that the $O_3 + O_2 + CO_2$ hydrate stored at 248 K or lower can preserve ozone at a mass fraction of 0.4–0.6% for over 20 days. In their study, an O_3 storage capacity as high as 0.91 mass% was obtained, which was the highest value ever reported.

Based on the van der Waals and Platteeuw theory,¹¹ the gas storage capacity in a hydrate has a positive correlation with the fugacity of the gas component. Nakajima *et al.*² experimentally confirmed that the O_3 storage capacity had no systematic dependence on the pressure. The thermodynamic model developed by Muromachi *et al.*¹ showed that the O_3 storage capacity in hydrates can be further extended by increasing the O_3 fraction in the gas phase. Based on these three reasons, it is necessary to increase the O_3 fraction in the feed gas to increase the O_3 storage capacity in the hydrates.

Since ozone easily decomposes to oxygen, it is difficult to control the O_3 fraction in the gas phase and accurately measure the O_3 fraction in the gas and hydrates. The O_3 fraction in the gas phase might not increase by simply increasing the $O_3 + O_2$ fraction in the $O_3 + O_2 + CO_2$ mixture because the O_3 decomposition reaction is accelerated under high O_3 density conditions. To demonstrate the increase in the O_3 fraction in the gas phase, it is necessary to measure the time evolution of the O_3 concentration in the feed gas in an increased range of the nominal $O_3 + O_2$ fraction. There is no report in the literature on the relationship between the O_3 concentration in the gas phase during hydrate formation and the O_3 storage capacity in the hydrates. There is still room for the improvement in the accurate measurement of the O_3 concentration in the gas and hydrates.

The major objectives of this study are to further increase the O_3 storage capacity in hydrates by increasing the O_3 fraction in the $O_3 + O_2 + CO_2$ feed gas and to better understand the relationship between the O_3 concentration in the gas phase and the O_3 storage capacity in the hydrates. To accurately specify the hydrate forming conditions, we first performed the phase equilibrium measurements for the $O_3 + O_2 + CO_2 + H_2O$ system exceeding the range covered by the previous study.¹⁰ The temperature range is from 272 K to 277 K and the pressure range is below 4 MPa for our three-phase equilibrium measurements. The molar ratios of ($O_3 + O_2$)-to- CO_2 or O_2 -to- CO_2 in the feed gas are approximately 4:6 and 5:5, respectively. To demonstrate the increase in the O_3 fraction in the gas phase, the time evolution of the O_3 concentration in the feed gas in the range of the nominal $O_3 + O_2$ mole fraction of 0.1–0.6 were measured. Based on the equilibrium data, we prepared the crystal samples of the $O_3 + O_2 + CO_2$ hydrates formed from three different $O_3 + O_2$ versus CO_2 molar ratios

(4:6, 5:5, 6:4) in the feed gas, monitoring the O_3 concentration in the gas phase in contact with the hydrates and measured the O_3 storage capacity. The improvements in the measurement of the O_3 storage capacity include sampling the formed hydrates at the low temperature of 253 K to avoid hydrate decomposition and the use of an air-tight container for mixing the hydrate sample into a potassium iodide aqueous solution to decrease the O_3 diffusion into the air.

Experimental

Materials

The fluid samples used in the experiments were deionized and distilled water: carbon dioxide of 99.995 vol% and oxygen of 99.9 vol% certified purity were provided by Japan Fine Products Corp., Kawasaki, Kanagawa Prefecture, Japan. The oxygen gas was used as received from the supplier to generate ozone with the aid of an ozone generator (ED-OG-R4DA, EcoDesign, Co., Ltd., Saitama Prefecture, Japan). For measuring the ozone concentration in each ozone-containing gas sample, we used an ultraviolet-absorptiometric ozone monitor (PG-620HA, Ebara Jitsugyo Co., Ltd., Tokyo, Japan).

Phase equilibrium measurements

We obtained the three-phase (gas + liquid + hydrate) equilibrium pressure versus temperature data for the ($O_3 + O_2 + CO_2 + H_2O$) systems. To demonstrate that ozone is clearly contained in the hydrate, we also measured the data for the ($O_2 + CO_2 + H_2O$) system corresponding to the experimental conditions of the O_3 -containing system and verified that the equilibrium pressure of the $O_3 + O_2 + CO_2 + H_2O$ systems is lower than that of the $O_2 + CO_2 + H_2O$ systems. This indicates that ozone can form a hydrate at a lower pressure than oxygen at a given temperature due to the preferential uptake of ozone into the hydrate compared to oxygen. The measurements were performed with the same setup as used in a previous study.¹⁰ Hydrates were formed in a vessel, which was a cylindrical stainless-steel chamber with 35 mm diameter, 120 mm height, and total volume of 190 cm³. The vessel was immersed in a temperature-controlled bath to maintain the temperature inside the vessel at a prescribed level. The pressure and temperature were measured by a strain-gauge pressure transducer (PHB-A-10MP, Kyowa Electronic Instruments Co., Ltd., Tokyo, Japan) and a platinum-wire resistance thermometer (NHRS1-0, Chino, Inc., Tokyo, Japan) connected to a resistance-measuring bridge. The expanded uncertainties in this study were estimated to be ± 0.05 K for the temperature, ± 6.0 kPa for the pressure and ± 0.0015 for the mole fraction of each species in the sampled gas with 95% coverage. We obtained the three-phase (gas + liquid + hydrate) equilibrium pressure versus temperature data for the $O_3 + O_2 + CO_2 + H_2O$ system and, for comparison, corresponding data for the $O_2 + CO_2 + H_2O$ system. Both experimental runs commenced by charging the vessel with 20 g of liquid water. For the $O_2 + CO_2 + H_2O$ system, we applied a temperature-search method.¹² The gas-mixing loop was charged with the $O_2 + CO_2$ mixture up to a prescribed level.



To induce hydrate nucleation, the vessel was immersed in the other bath in which the coolant was cooled to ~ 253 K. After the temperature of the vessel was decreased to ~ 263 K, the vessel was reconnected to the setup. Once the hydrate formation was detected during this cooling process, the temperature was increased in steps of 0.1 K. Responding to the stepwise increase in temperature, the pressure also increased stepwise. This process of the stepwise temperature rise was continued until the completion of the hydrate dissociation. The point at which the slope of the p - T data plots sharply changes was determined to be the hydrate dissociation point. This is the three-phase equilibrium point. After readjusting the system temperature to the level of the equilibrium conditions, we then performed the gas-sampling procedure.

For the $O_3 + O_2 + CO_2 + H_2O$ system, we applied a modified pressure-search method.¹⁰ To quickly form hydrates, we performed the above-mentioned cooling before the gas charging process. The gas-mixing loop was charged with the $O_3 + O_2$ mixture to a pressure of 0.3 MPa by the ozone generator. For measurements at higher system pressures, we prepared a gas pressurizer in which the $O_3 + O_2$ gas supplied from the ozone generator could be compressed up to 2.5 MPa by a water column displaced by the oxygen gas cylinder. The mixture was pressurized by the gas pressurizer equal (on a molar basis) to that of the pure O_2 gas supplied to the vessel in the corresponding experiment for the $O_2 + CO_2 + H_2O$ system. The mixture was charged with CO_2 gas until the system pressure increased to the equilibrium pressure. The uncertainties of the molar feed ratios of CO_2 to $O_3 + O_2$ corresponded to that of the pressure measurements. They are estimated to be ± 0.016 for the molar feed ratios of CO_2 to $O_3 + O_2$ with 95% coverage. It was determined in the corresponding experiment for the $O_2 + CO_2 + H_2O$ system performed at the same temperature. We measured the temperature and visually confirmed the melting of the ice phase during the hydrate-phase growth process. We defined the system conditions at the stage when a pressure increase (~ 3 kPa) from its minimum value was observed as the thermodynamic phase-equilibrium conditions. The gas-sampling procedure generally followed that which was used for the $O_2 + CO_2 + H_2O$ system. We separated the gas-sampling section from the test cell by closing the valves between them. We discharged the gas in the former section into the gas-sample holder to ~ 500 kPa. The residual gas in the gas-sampling section was immediately injected into the ozone monitor. The gas-sample holder was then heated to completely decompose the ozone to oxygen. The resultant $O_2 + CO_2$ mixture in the holder was subjected to gas-chromatographic analysis to determine the O_2 versus CO_2 molar ratio in the feed gas.

O_3 storage capacity measurements

Fig. 1 shows a schematic of the apparatus used for the formation experiments of the $O_3 + O_2 + CO_2$ hydrates. The time evolution measurements of the O_3 concentration in the feed gas were performed in the gas-mixing chamber, which was immersed in a water bath temperature-controlled at 280 K. The setup was flushed at least five times with pure O_2 gas, then evacuated. After confirming that the O_3 fraction in the gas

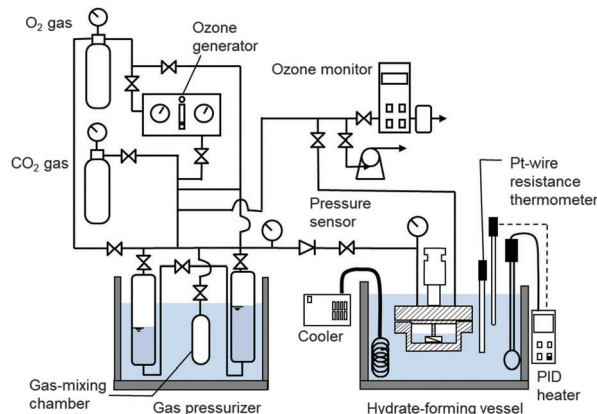


Fig. 1 Schematic of the experimental setup for determining the ozone storage capacity in hydrates.

mixture released from the O_3 generator was in the range 0.10–0.12, a gas-mixing chamber and a gas pressurizer were charged with the $O_3 + O_2$ mixture gas to a pressure of 0.3 MPa. The mixture was pressurized by the gas pressurizer until the pressure inside the vessel increased to the prescribed level. Subsequently, CO_2 gas was supplied to the gas mixing chamber until the pressure inside increased to 3.5 or 4.0 MPa.

The $O_3 + O_2 + CO_2$ hydrate samples were formed in the hydrate-forming vessel, which was charged with 30 g of water and immersed in a bath of an aqueous ethylene glycol solution temperature-controlled at 272 K. The $O_3 + O_2 + CO_2$ feed gas for forming the hydrates was mixed by the same procedure as mentioned above. The $O_3 + O_2 + CO_2$ gas mixture was supplied to the hydrate-forming vessel until the pressure inside the vessel increased to the prescribed level (2.5 or 3.0 MPa). A series of intermittent batch operations for forming the hydrates were then started by turning on the stirrer in the vessel. To prevent the system pressure from significantly decreasing from the prescribed level, additional feed gas was supplied by the gas-mixing chamber every 20 minutes.

To minimize the change in composition of the gas mixture inside the hydrate-forming vessel, the residual gas inside the vessel was discharged to a pressure of 2.5 MPa every hour and the fresh gas was charged to 3.0 MPa from the gas-mixing chamber. Also, to monitor the O_3 concentration in the gas phase in contact with the hydrates, the discharged gas was injected into the O_3 monitor to measure the O_3 concentration in the gas phase. These batch and gas-exchange operations were repeated several times until no decrease in the system pressure was observed during each batch operation and hence we judged that the hydrate formation had ceased. The hydrate sample was then retrieved from the vessel at a temperature below 215 K and under a dry nitrogen-gas atmosphere. Small portions of the hydrate were sampled for an iodometric measurement to determine its initial O_3 storage capacity. To experimentally improve the measurement of the O_3 storage capacity, we sampled the formed hydrates at a temperature of 253 K and used an air-tight container to mix the hydrate samples in potassium iodide to avoid ozone diffusion into the air.



An O₃ + O₂ + CO₂ hydrate sample was subjected to powder X-ray diffraction (PXRD) measurements to confirm its crystallographic structure and, at the same time, to examine the fraction of the condensed water phase inevitably included in the sample. The sample was finely powdered under a dry N₂ gas atmosphere at a temperature comparable to liquid N₂ (~100 K), then top-loaded on a copper (Cu) specimen holder. The PXRD measurements were done using Cu-K α radiation generated by an Ultima III diffraction system (Rigaku Corp., Tokyo, Japan). Analyses of the lattice constant of the hydrate and mass fractions of any unreacted solid water (ice) in the samples were performed by the Rietveld method using the RIETAN-FP program.¹³

Results and discussion

Phase equilibrium measurements

The phase equilibrium pressure *versus* temperature data measured for the (O₃ + O₂ + CO₂ + H₂O) and (O₂ + CO₂ + H₂O) systems in the present study are compiled in Table 1. These are not only the *p* and *T* values, but also the relevant values of the mole fractions, *y*, of O₃, O₂ and CO₂ in the gas mixture discharged from the gas-sampling cylinder. The *p*–*T* data that we obtained may be characterized by two groups in reference to the nominal value of *y*_{CO₂} (0.6 or 0.5). These data are plotted in Fig. 1 with the previously reported data having the nominal value of *y*_{CO₂} (0.9, 0.8 and 0.7)¹⁰ for comparison. As presented in Fig. 2, the equilibrium pressures corresponding to the equilibrium temperatures from 272 to 279 K ranged from 1.56 to 2.91 MPa for the O₃ + O₂ + CO₂ + H₂O system. There was some scatter in the gas-phase composition in

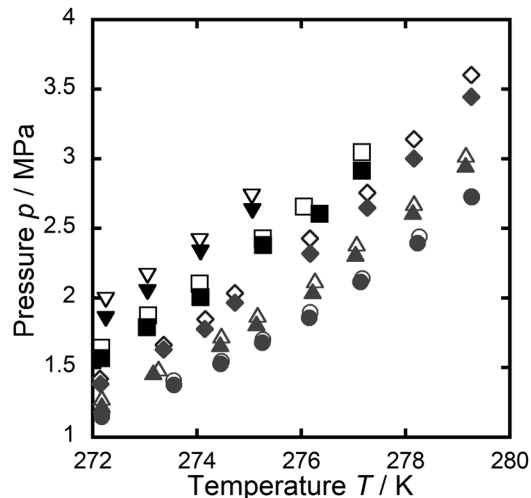


Fig. 2 Three-phase equilibrium *p*–*T* data for the O₃ + O₂ + CO₂ + H₂O system (●, ▲, ◆, ■, ▼) and the O₂ + CO₂ + H₂O system (○, △, ◇, □, ▽). The details of the three gas mole fractions are specified in Table 1. The data points relevant to the five different levels of *y*_{CO₂}, the CO₂ mole fraction in the gas phase, are denoted by their geometries as follows: circles (●, ○) for *y*_{CO₂} ≈ 0.9; triangles (▲, △) for *y*_{CO₂} ≈ 0.8; rhombuses (◆, ◇) for *y*_{CO₂} ≈ 0.7; and squares (■, □) for *y*_{CO₂} ≈ 0.6; triangles (▼, ▽) for *y*_{CO₂} ≈ 0.5. The data for *y*_{CO₂} ≈ 0.6 and *y*_{CO₂} ≈ 0.5 were newly obtained in this study. The other data were obtained in our previous study.¹⁰

each group because the O₃ composition in the gas phase in contact with the formed hydrate may change from that in the feed gas due to the ozone-to-oxygen reaction. The scatter is also partially ascribed to the gas-compositional fractionation during hydrate formation. However, we found that the *p*–*T* data points are aligned on a single smooth curve. These data have consistent tendencies with the previous study, that is, the equilibrium pressure decreases with increasing *y*_{CO₂} at a given temperature. These data also show that even a small fraction of ozone (*y*_{O₃} ≈ 0.025 to 0.03) partially replacing oxygen causes an equilibrium pressure decrease of ~0.14 MPa.

O₃ storage capacity measurements

To better understand the relationship between the feed O₃ + O₂ fraction *y*_{O₃+O₂,feed} and feed O₃ concentration *Y*_{O₃,feed}, we measured the time evolution of *Y*_{O₃,feed} in the *y*_{O₃+O₂,feed} range 0.1–0.6 as plotted in Fig. 3.

As seen in Fig. 3, *Y*_{O₃,feed} is increased at the higher *y*_{O₃+O₂,feed} but at the same time, the O₃ decomposition rate is also increased due to the increase in the partial pressure of the O₃ + O₂ gas. To maintain the higher *Y*_{O₃,feed} through hydrate formation, the nominal *y*_{O₃+O₂,feed} of 0.4–0.6 are suitable to reach a compromise between the effects of the initial *Y*_{O₃,feed} increase and O₃ decomposition rate. A further increase in *Y*_{O₃,feed} is not expected even if *y*_{O₃+O₂,feed} is higher than 0.7.

Based on the phase equilibrium data obtained in this study, the thermodynamic conditions to form hydrate samples for the O₃ density measurements were specified. We performed O₃ + O₂ + CO₂ hydrate-forming experiments under the thermodynamically more stable conditions (*i.e.*, lower temperature/higher pressure than the equilibrium conditions).

Table 1 Three-phase equilibrium *p*–*T* data for the O₃ + O₂ + CO₂ + H₂O and O₂ + CO₂ + H₂O systems

Feed compositions Nominal value (mean value) of <i>y</i> _{CO₂}	Equilibrium conditions				
	<i>T</i> /K	<i>p</i> /MPa	<i>y</i>		
O ₃			O ₂	CO ₂	
≈ 0.6	277.2	2.914	0.027	0.386	0.587
	276.6	2.605	0.017	0.332	0.651
	275.3	2.379	0.019	0.392	0.589
	274.1	2.007	0.031	0.383	0.587
	273.0	1.790	0.030	0.381	0.588
	272.2	1.567	0.030	0.382	0.588
	277.2	3.047	—	0.398	0.602
	276.1	2.656	—	0.376	0.624
	275.3	2.427	—	0.407	0.593
	274.1	2.104	—	0.415	0.585
273.1	1.876	—	0.405	0.595	
272.2	1.643	—	0.380	0.620	
≈ 0.5	275.1	2.626	0.022	0.477	0.501
	274.1	2.328	0.029	0.441	0.530
	273.1	2.045	0.027	0.471	0.502
	272.3	1.850	0.028	0.451	0.521
	275.1	2.730	—	0.499	0.501
	274.1	2.409	—	0.494	0.506
	273.1	2.162	—	0.494	0.506
	272.3	1.988	—	0.501	0.499



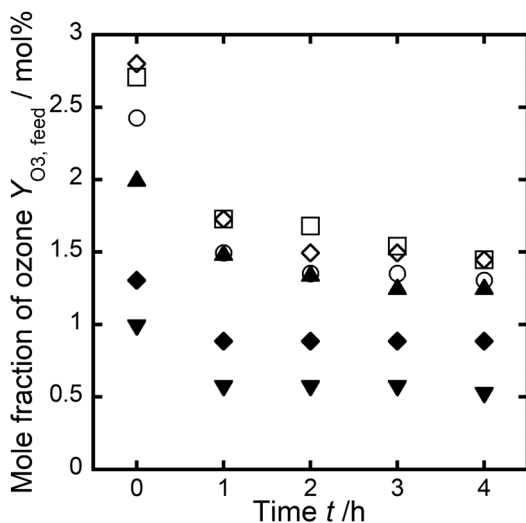


Fig. 3 The time evolution of $Y_{O_3,feed}$ in the range of $y_{O_3+O_2,feed}$ 0.1–0.6. (\blacktriangledown , \blacklozenge , \blacktriangle , \circ , \square , \diamond) $y_{O_3+O_2,feed} \approx 0.1, 0.2, 0.3, 0.4, 0.5, 0.6$.

The hydrates were formed from a mixture of $O_3 + O_2$ and CO_2 in an approximately 4:6, 5:5 and 6:4 molar ratio in the feed gas at a system pressure p of 2.5 or 3.0 MPa and a temperature T of 272 K. The hydrates formed in each experiment were then subjected to an iodometric measurement to determine their O_3 storage capacity $X_{O_3,hyd}$.

The system pressure dependencies on $X_{O_3,hyd}$ are shown in Fig. 4, which also includes the data measured by Nakajima *et al.*² Similar to their data, $X_{O_3,hyd}$ shows no dependence on the system pressure. In comparison with their data at the same $y_{O_3+O_2,feed}$ of 0.4, the data obtained in this study show a higher value of $X_{O_3,hyd}$. This increase in $X_{O_3,hyd}$ is ascribed to the improvements in the measurement of the O_3 storage capacity.

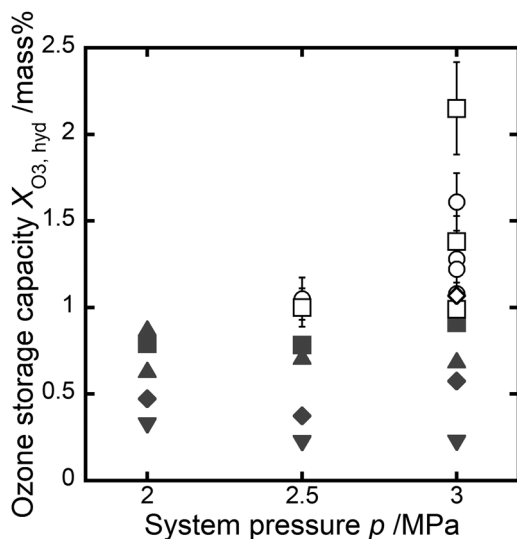


Fig. 4 $X_{O_3,hyd}$ versus the system pressure p . These data were characterized by $y_{O_3+O_2,feed}$: (\blacktriangledown , \blacklozenge , \blacktriangle , \blacksquare) $y_{O_3+O_2,feed} \approx 0.1, 0.2, 0.3, 0.4$; (\circ , \square , \diamond) $y_{O_3+O_2,feed} \approx 0.4, 0.5, 0.6$ [this study]. The error bar for each data point represents the uncertainty of the O_3 fraction measurement by iodometry.

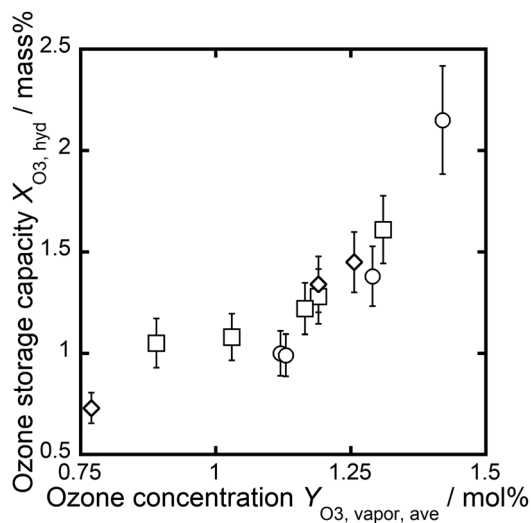


Fig. 5 $X_{O_3,hyd}$ versus $Y_{O_3,vapor,ave}$. These data were characterized by $y_{O_3+O_2,vapor}$: (\square , \circ , \diamond) $y_{O_3+O_2,vapor} \approx 0.4, 0.5, 0.6$. The error bar for each data point represents the uncertainty of the O_3 fraction measurement by iodometry.

The highest value of $X_{O_3,hyd}$ in this study was ~ 2.15 mass%, which was 2.36 times higher than the highest past record of 0.91 mass%.

We then showed the relationship between the O_3 concentration in the gas phase $Y_{O_3,vapor}$ and the O_3 storage capacity in the hydrates. Since $Y_{O_3,vapor}$ decreases with time, we define $Y_{O_3,vapor,ave}$, the time average of $Y_{O_3,vapor}$, to represent “the mole concentration of ozone in the gas phase in contact with the hydrate”. The relationship between $X_{O_3,hyd}$ and $Y_{O_3,vapor,ave}$ is depicted in Fig. 5. This figure shows that $X_{O_3,hyd}$ is well correlated with $Y_{O_3,vapor,ave}$. At $Y_{O_3,vapor,ave} = 0.77$ mol%, $X_{O_3,hyd}$ is 0.73 mass%. $X_{O_3,hyd}$ increases with increasing $Y_{O_3,vapor,ave}$. The greatest value of $X_{O_3,hyd}$ is 2.15 mass% at $Y_{O_3,vapor,ave} = 1.42$ mol%.

The highest recorded value of $X_{O_3,hyd}$, as high as 2.15 mass%, was not obtained by the hydrates formed from the mixture of $O_3 + O_2$ and CO_2 in an approximately 6:4 ratio, but from the 5:5 molar ratio in the feed gas. This may be appear strange because there should be a positive correlation tendency between $y_{O_3+O_2,vapor}$ and $X_{O_3,hyd}$ as observed in the previous study.² This apparent inconsistency is explained by carefully measuring $Y_{O_3,vapor}$.

That is, the results demonstrate the increase in $X_{O_3,hyd}$ was not controlled by the nominal value of $y_{O_3+O_2,vapor}$, but by the actual concentration of ozone in the gas phase in contact with hydrate represented by $Y_{O_3,vapor,ave}$. In comparison to the highest past $X_{O_3,hyd}$ value of 0.91 mass%, the increase to 2.15 mass% resulted from accurate measurement of $X_{O_3,hyd}$ by improving the method of the O_3 storage capacity measurement and increasing the mole fraction of ozone in the gas phase in contact with the hydrate during the hydrate formation by increasing the $y_{O_3+O_2,vapor}$ from 0.4 to 0.5.

Fig. 6 shows a PXRD pattern (measured at 98 K) of an $O_3 + O_2 + CO_2$ hydrate formed from a $O_3 + O_2$ and CO_2 mixture in an



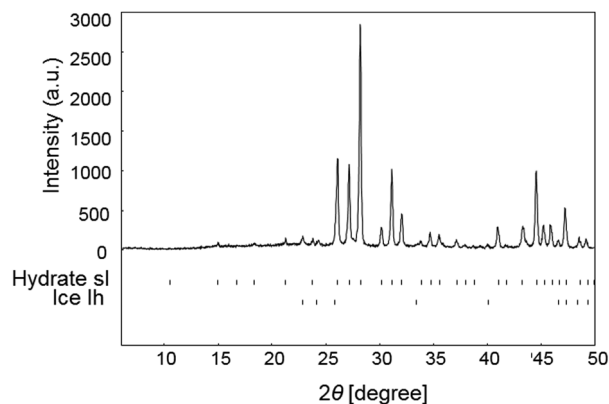


Fig. 6 PXRD pattern of an $O_3 + O_2 + CO_2$ hydrate at 98 K. Upper and lower tick patterns correspond to the structure I hydrate and hexagonal ice, respectively. The hydrate sample (accompanied by ice crystals) used in this PXRD measurement was formed from a mixture of $O_3 + O_2$ and CO_2 in a nearly 6 : 4 molar ratio under the conditions of $p = 3.0$ MPa and $T = 272$ K.

apparently 6 : 4 molar ratio at a system pressure p of 3.0 MPa and a temperature T of 272 K. This pattern indicates that the hydrate sample used here was a mixture of a hydrate in structure I with a lattice constant of 11.8223(4) Å and hexagonal ice, Ih with a mass fraction of 0.01. The lattice constant of the $O_3 + O_2 + CO_2$ hydrate in this study is in good agreement with that of the $O_3 + O_2 + CO_2$ hydrate with a lower O_3 gas capacity in the previous study.² The increase in the O_3 gas storage capacity does not affect the host structure of the gas hydrate. This result indicates the high stability of O_3 within the host water cages even for the higher O_3 capacity obtained in this study.

Conclusions

The three-phase equilibrium p - T data for the $O_3 + O_2 + CO_2 + H_2O$ and $O_2 + CO_2 + H_2O$ systems were measured within the temperature range from 272 K to 277 K, corresponding to pressures from 1.6 MPa to 3.1 MPa, for each of the two different ($O_3 + O_2$)-to- CO_2 or O_2 -to- CO_2 molar ratios in the feed gas, which are approximately 4 : 6 and 5 : 5.

The O_3 storage capacity in the $O_3 + O_2 + CO_2$ hydrates was successfully increased by increasing the O_3 concentration in the gas phase and improving the experimental procedure. The highest O_3 storage capacity in this study was ~ 2.15 mass%,

which was 2.36 times higher than the highest past record of 0.91 mass%.

New findings in this study are the hydrate forming conditions as well as the relationship between $Y_{O_3, \text{vapor, ave}}$ and $X_{O_3, \text{hyd}}$ and the highest $X_{O_3, \text{hyd}}$. Based on these findings, the required $Y_{O_3, \text{vapor, ave}}$ to obtain the desired $X_{O_3, \text{hyd}}$ could be predicted.

Acknowledgements

This study was supported in part by JKA through promotion funds from KEIRIN RACE. A part of this study was performed and Keio University. The authors are indebted to Mr Ozaki, Mr Tomura and Mr Nishi of IPC for their encouragement. The financial support by IPC is also greatly appreciated.

Notes and references

- 1 S. Muromachi, H. D. Nagashima and R. Ohmura, *J. Chem. Thermodyn.*, 2013, **64**, 193–197.
- 2 T. Nakajima, T. Kudo, R. Ohmura, S. Takeya and Y. H. Mori, *PLoS One*, 2012, **7**, 1–6.
- 3 Kurita Water Industries Ltd., *JP Pat.*, 2007-210881, 2007.
- 4 O. S. Subbotin, T. P. Adamova, R. V. Belosludov, H. Mizuseki, Y. Kawazoe and V. R. Belosludov, *J. Struct. Chem.*, 2012, **53**, 627–633.
- 5 G. McTurk and J. G. Waller, *Nature*, 1964, **202**, 1107.
- 6 S. Imai, K. Okutani, R. Ohmura and Y. H. Mori, *J. Chem. Eng. Data*, 2005, **50**, 1783–1786.
- 7 S. Muromachi, T. Nakajima, R. Ohmura and Y. H. Mori, *Fluid Phase Equilib.*, 2011, **305**, 145–151.
- 8 S. Muromachi, R. Ohmura, S. Takeya and Y. H. Mori, *J. Phys. Chem. B*, 2010, **114**, 11430–11435.
- 9 T. Nakajima, S. Akatsu, R. Ohmura, S. Takeya and Y. H. Mori, *Angew. Chem., Int. Ed.*, 2011, **50**, 1–5.
- 10 S. Muromachi, R. Ohmura and Y. H. Mori, *J. Chem. Thermodyn.*, 2012, **49**, 1–6.
- 11 J. H. van der Waals and J. C. Platteeuw, *Adv. Chem. Phys.*, 1959, **2**, 1–57.
- 12 A. Danesh, B. Tohidi, R. W. Burgass and A. C. Todd, *Chem. Eng. Res. Des.*, 1994, **72**, 197–200.
- 13 F. Izumi and K. Momma, *Solid State Phenom.*, 2007, **130**, 15–20.

